Modeling and Robust Control of a Grid Connected Direct Driven PMSG Wind Turbine By ADRC

Imad ABOUDRAR, Soumia EL HANI, Hamza MEDIOUNI, Ahmed AGHMADI

Energy Optimization, Diagnosis and Control, Centre de Recherche en Sciences et Techniques de l'Ingenieur et de la Sante, l'Ecole Normale Superieure de l'Enseignement Technique (ENSET), Mohammed V University, Rabat, Morocco

imad.aboudrar@um5s.net.ma, s.elhani@um5s.net.ma, hamzamediouni16@gmail.com, ahmed.aghmadi@gmail.com

DOI: 10.15598/aeee.v16i4.2952

Abstract. *In this paper, we present the modeling and control of a grid connected Variable Speed Wind Energy Conversion System (VS-WECS) based on a Direct Driven Permanent Magnet Synchronous Generator (DD-PMSG). A new robust control has been proposed and utilized to operate the wind turbine so as to extract the maximum power from the wind energy and to ensure a unit power factor. This control is known as the Active Disturbance Rejection Control (ADRC) and it is based on the Extended State Observer (ESO). It consists in controlling, through the stator currents, the machine side converter in order to adapt the rotational speed of the generator to the different wind speed profiles (Maximum Power Point Tracking MPPT). In addition, it ensures the control of the DC bus voltage and the exchange of active and reactive powers between the wind turbine and the electrical power grid.*
In order to evaluate the performance of the proposed control a series of simulations are made under the MATLAB/SIMULINK environment.
The results obtained by simulation show that the proposed strategy is efficient in terms of stability and precision as well as for the robustness with regard to the internal disturbances when variying the parameters of the machine.

Keywords

ADRC, ESO, MPPT, PLL, PMSG, wind turbine.

1. Introduction

In recent years, energy consumption is one of the biggest concerns because it is increasing in all its forms and it is associated with polluting effects, mainly caused by burning the fossil fuels (oil, gas, and coal). Facing up to these problems, several countries are turning to a new form of energy which is clean and inexhaustible "renewable energy" [1].

Among renewable energy sources, wind energy has the most significant energy potential and a relatively low cost of production, leading to a growing development of this sector on a global scale. Wind energy worldwide is increasing every year and production capacity has increased by a factor of 6.5 over the past ten years [2].

The total energy extracted from the wind depends not only on the incident wind speed, but also on the control applied to the WECS. Generally, the extraction of maximum wind power is achieved by using fully controlled variable speed wind turbine generators. The wind turbine rotational speed is regulated according to the incident wind speed to track the maximum wind power trajectory [3]. As a grid-connected power generation system, the wind turbine generator must have the ability to control the active and reactive powers injected to the grid. Variable speed wind turbine topologies comprise many different converters configurations, based on efficiency, cost, yearly energy capturing and the overall system control complexity [4]. Permanent Magnet Synchronous Generators (PMSG) based variable speed wind turbines are considered as a suitable and practical technology in wind generation industry since they are self-excited, and thus permit high efficiency operations [5]. Additionally, the gearbox can be omitted owing to its capability of working at low rotational speed; or in other WECSs, the gearbox is one of the most critical mechanisms, as its failure is extremely expected, and, therefore, it requires careful and regular maintenance [6]. In this context, the present article describes an exploitation of a PMSG based wind turbine.

Researchers are continuing to carry out investigations in order to improve the electromechanical conversion efficiency and the energy supplied quality. For PMSG variable speed WECS based on back-to-back converters, the power delivery is often controlled over the grid-side converter by using a PI controller [7] and [8]. However, it does not guarantee a zero steady-state error while controlling the currents, which is due to the presence of cross-coupling terms between d-q axis components, which results in an inappropriate power delivery [9].

In recent years, several publications have appeared documenting the application of the Active Disturbance Rejection Control (ADRC), which was originally proposed by Jinqgin Han [10] and [11]. The prospective of ADRC as an effective new control strategy is evident in many case studies, where the technique is used to adress a number of benchmark problems in diverse industry sectors, with promising results. However, to the authors best knowledge, very few publications are available in the literature that address the issue of controlling the PMSG wind energy conversion systems. In [12], the authors have proposed a predictive ADRC to overcome the time delay in wind turbine systems, and in [13], the authors have proposed an optimal MPPT control for parameters tuning based on optimization algorithms. Finally, in [14] the authors have discussed the rejection of lumped disturbance, including the system uncertainties in the internal dynamics and unknown external forces.

Our contribution in this paper is to develop a new robust control strategy for the grid connected based PMSG wind turbine by ADRC to extract the maximum power available from the turbine blades and to regulate the power delivery. For this purpose, this paper is structured as follows: the second chapter presents a general modeling of the wind energy conversion chain. The third chapter introduces the mathematical model of the Active Disturbance Rejection Controller. The fourth one gives the machine and the grid side converters control by ADRC while in the fifth chapter, the simulation results of the wind energy conversion system are presented.

2. Modeling of the DD-PMSG Wind Turbine Systems

In this chapter, we are interested in modeling all the wind energy conversion chain components, going from the wind kinetic energy conversion into mechanical energy to the connection with the power grid.

The studied system is shown in Fig. 1, and it consists of:

- A three-bladed, horizontal-axis wind turbine operating at different wind conditions allowing us to convert the kinetic energy into mechanical energy.
- A permanent magnetic synchronous generator with a nominal power of 750 KW that converts the mechanical energy into electrical energy.
- Two back to back converters (Machine side and Grid side Converters) interconnected via a DC bus that allows the power exchange.
- A three-phase RL filter, which connects the converters to the electrical utility grid and reduces the current total harmonics distortion.

2.1. Wind Turbine Modeling

The turbine converts the aerodynamic energy of the wind into mechanical energy. Its modeling consists in expressing the extracted power P_{aero} as a function of the incident wind speed V and the operating conditions. It is expressed by:

$$P_{aero} = C_p\left(\lambda, \beta\right) P_w = C_p\left(\lambda, \beta\right) \frac{\rho s v^3}{2}. \tag{1}$$

Its aerodynamic torque T_{aero} is given by the following expression:

$$T_{aero} = \frac{1}{2\Omega_t} C_p\left(\lambda, \beta\right) \rho s v^3, \tag{2}$$

where ρ is the air density, generally taken equal to 1.225 kg·m^{-3}.

The wind turbine aerodynamic efficiency is represented by a power factor called C_p [15]. This coefficient depends on the turbine characteristics (speed ratio λ and pitch angle β). Figure 2 shows the change of C_p for different values of β .

$$C_p\left(\lambda, \beta\right) = 0.5176\left(\frac{116}{\lambda'} - 0.4\beta - 5\right) e^{\frac{-21}{\lambda'}} + 0.0068\lambda, \tag{3}$$

$$\lambda = \frac{\Omega_t R}{V}, \tag{4}$$

$$\frac{1}{\lambda'} = \frac{1}{\lambda + 0.08\beta} - \frac{0.035}{\beta^3 + 1}, \tag{5}$$

where Ω_t is the turbine rotational speed.

The mechanical equation of the turbine shaft which is rigidly connected to the synchronous generator is given by:

$$J \frac{\mathrm{d}\Omega_t}{\mathrm{d}t} = T_{aero} - T_{em} - f\Omega_t, \tag{6}$$

where J is the system total inertia, f is the friction coefficient and T_{em} represents the generator electromagnetic torque.

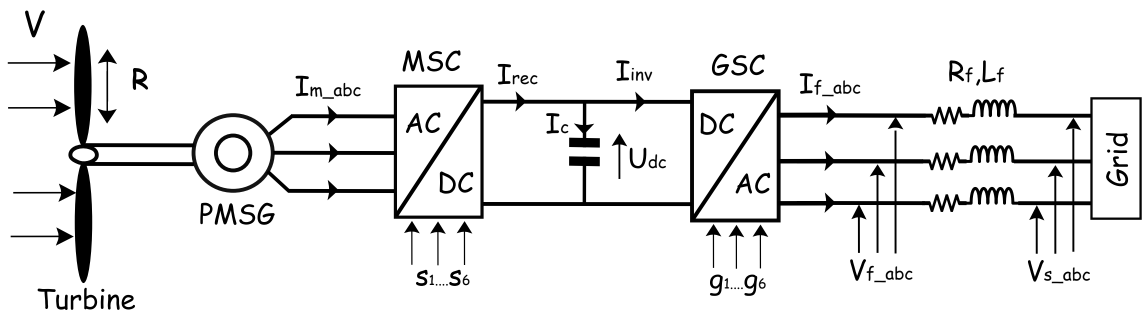

Fig. 1: Grid-connected variable speed wind energy conversion system based on permanent magnet synchronous generator.

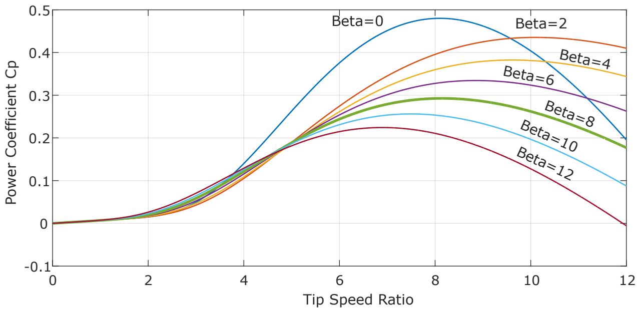

Fig. 2: Power coefficient characteristics for various values of pitch angle β.

2.2. Permanent Magnet Synchronous Generator Modeling

The PMSG dynamic model in the d-q frame is presented by:

$$V_d = -(R_s + pL_d)i_d + \omega_e L_q i_q, \tag{7}$$

$$V_q = -(R_s + pL_q)i_q - \omega_e L_d i_d + \omega_e \psi_f, \tag{8}$$

$$T_{em} = \frac{3}{2} P \left[(L_d - L_q) i_d i_q + i_q \psi_f \right]. \tag{9}$$

R_s represents the stator resistance, L_d and L_q are the direct and quadrature inductances, i_d and i_q are the stator currents in the d-q frame, ψ_f is the permanent magnet flux, and P are pair poles [15].

ω_e is the PMSG speed and it is given by:

$$\omega_e = P\Omega_t. \tag{10}$$

2.3. Modeling of The Back to Back Converters

The wind energey conversion chain studied in this work consists of two converters coupled on a common DC bus. They are bidirectional and consist of IGBT's power transistors associated with antiparallel diodes and controlled by Pulse Width Modulation (PWM).

The machine side converter is used to control the generator torque and speed while the grid side converter regulates the DC bus voltage and ensures the delivery of the produced active power to the main power grid.

Both converters are identical and can be used in both inverter and rectifier mode. Here we present the modeling of the grid side converter.

The modulated voltages are given by:

$$\begin{cases} V_{f-a} = \dfrac{2s_{11} - (s_{12} + s_{13})}{3} U_{dc}, \\ V_{f-b} = \dfrac{2s_{12} - (s_{11} + s_{13})}{3} U_{dc}, \\ V_{f-c} = \dfrac{2s_{13} - (s_{11} + s_{12})}{3} U_{dc}. \end{cases} \tag{11}$$

The modulated current I_{inv} is given by:

$$I_{inv} = s_{11} i_{fa} + s_{12} i_{fb} + s_{13} i_{fc}. \tag{12}$$

Applying Park's transformation, Eq. (11) and Eq. (12) become as follows:

$$\begin{cases} V_{fd} = s_d U_{dc}, \\ V_{fq} = s_q U_{dc}. \end{cases} \tag{13}$$

$$I_{inv} = s_d i_{fd} + s_q i_{fq}. \tag{14}$$

2.4. DC Link and Filter Modeling

The connection of the energy conversion system with the electrical power grid is carried out via a RL filter (L_f, R_f), It is used to prevent harmonic currents from spreading through the electrical power grid:

$$\begin{cases} V_{s-a} = V_{fa} - R_f i_{fa} - L_f \frac{\mathrm{d}i_{fa}}{\mathrm{dt}}, \\ V_{s-b} = V_{fb} - R_f i_{fb} - L_f \frac{\mathrm{d}i_{fb}}{\mathrm{dt}}, \\ V_{s-c} = V_{fc} - R_f i_{fc} - L_f \frac{\mathrm{d}i_{fc}}{\mathrm{dt}}. \end{cases} \tag{15}$$

Applying Park's transformation, Eq. (15) becomes in d-q frame as follows:

$$\begin{cases} V_{gd} = V_{fd} - R_f i_{fd} - L_f \frac{\mathrm{d}i_{fd}}{\mathrm{dt}} + L_f \omega_g i_{fq}, \\ V_{gq} = V_{fq} - R_f i_{fq} - L_f \frac{\mathrm{d}i_{fq}}{\mathrm{dt}} - L_f \omega_g i_{fd}, \end{cases} \tag{16}$$

where v_{fd}, v_{fq} are the inverter voltage components, v_{gd}, v_{gq} are the grid voltages and i_{fd}, i_{fq} are the filter currents.

The modeling of DC Link Voltage is given by:

$$\frac{\mathrm{d}U_{dc}}{\mathrm{d}t} = \frac{1}{C}(i_{rec} - i_{inv}), \tag{17}$$

where C is the DC link Capacitor.

3. Active Disturbance Rejection Control

3.1. Mathematical Model of ADRC

ADRC is a robust control strategy proposed by Jingqing Han in 2009 [16], it mainly consists of three parts: Tracking Differentiator (TD), Extended State Observer (ESO), and Non-Linear State Error Feedback (NLSEF). The block diagram of a first order standard ADRC is shown in Fig. 3.

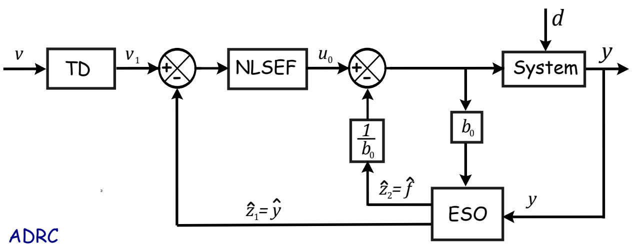

Fig. 3: Block diagram of a first order Active Disturbance Rejection Controller.

In Fig. 3, v is the input signal, v_1 is the input tracking signal; y is the system feedback signal; z_1 is the estimated tracking signal; z_2 is the total disturbances estimation; b_0 is the compensation factor; z_2/b_0 is the internal and external disturbances compensation; u_0 is the initial control object by NLSEF; u is the final control signal after disturbance compensation.

For a first-order controlled object, its mathematical model of ADRC is set as [17]:

$$\begin{cases} \varepsilon_0 = v_1 - v, \\ \dfrac{\mathrm{d}v_1}{\mathrm{d}t} = -rfal(\varepsilon_0, \alpha_0, \delta_0). \end{cases} \tag{18}$$

$$\begin{cases} \varepsilon = z_1 - y, \\ \dfrac{\mathrm{d}z_1}{\mathrm{d}t} = z_2 - \beta_{01} fal(\varepsilon, \alpha, \delta) + bu(t), \\ \dfrac{\mathrm{d}z_2}{\mathrm{d}t} = \beta_{02} fal(\varepsilon, \alpha, \delta). \end{cases} \tag{19}$$

$$\begin{cases} \varepsilon_1 = v_1 - z_1, \\ u_0 = \beta_1 fal(\varepsilon_1, \alpha_1, \delta_1), \\ u = u_0 - \dfrac{z_2}{b_0}. \end{cases} \tag{20}$$

$$fal(\varepsilon, \alpha, \delta) = \begin{cases} |\varepsilon|^{\alpha} sgn(\varepsilon) & |\varepsilon| > \delta, \\ \dfrac{\varepsilon}{\delta^{1-\alpha}} & |\varepsilon| \le \delta, \end{cases} \tag{21}$$

where the mathematical model of the TD is defined by Eq. (18). The model of ESO is given by Eq. (19), and for NLSEF block it is represented by Eq. (20). β_{01},β_{02},β_1 are output error factors, $fal(\varepsilon, \alpha, \delta)$ is the best function which is defined by Eq. (21), δ is the filtering factor to ESO, and α is a nonlinear factor.

In practice, the ADRC controller needs to adjust a large number of parameters and adjusting these parameters is complicated. So as to reduce the model complexity and the controller computational, a Linear ADRC design method is proposed and applied to the DD-PMSG Wind Energy Conversion System.

3.2. Linear ADRC Design

The LADRC consists of a proportional controller and an ESO [18]. The uncertainties of the system and the external disturbances are considered as a generalized disturbance. The ESO is used to estimate the system states and the generalized disturbance. The proportional controller drives the tracking error between the output of the system and the reference signal to zero. The block diagram of a first order LADRC is depicted in Fig. 4.

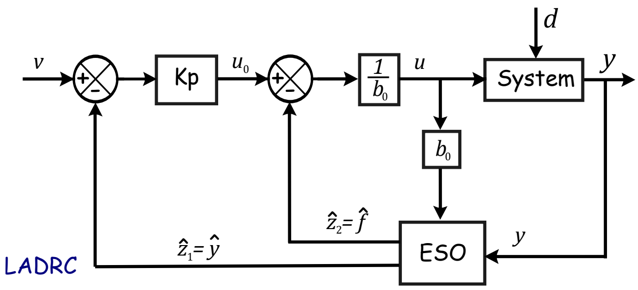

Fig. 4: Block diagram of a first order Linear ADRC.

Considering a First Order System where the plant dynamics is given by:

$$\frac{\mathrm{d}y(t)}{\mathrm{d}t} = -\frac{1}{T}y(t) + bu(t). \tag{22}$$

External disturbance $d(t)$ can be added to the process by replacing b with $b = b_0 + \Delta b$, where b_0 will characterise the system known part and Δb, the (unknown) modeling errors part.

$$\begin{aligned} \frac{\mathrm{d}y(t)}{\mathrm{d}t} &= -\frac{1}{T}y(t) - \frac{1}{T}d(t) + b_0u(t) + \Delta bu(t) \\ &= f(y, d, t) + b_0u(t), \end{aligned} \tag{23}$$

where $f(y, d, t)$ represents the system general total disturbances.

Let $x_1 = y$, $x_2 = f$, and $\dot{f} = h$.

The process state-space model is presented by:

$$\begin{cases} \dot{x} = Ax + Bu + Eh, \\ y = Cx. \end{cases} \tag{24}$$

with: $A = \begin{bmatrix} 0 & 1 \\ 0 & 0 \end{bmatrix}$, $B = \begin{bmatrix} b \\ 0 \end{bmatrix}$, $C = \begin{bmatrix} 1 & 0 \end{bmatrix}$, $E = \begin{bmatrix} 0 \\ 1 \end{bmatrix}$, $x = \begin{bmatrix} x_1 \\ x_2 \end{bmatrix}$.

The Linear Extended State Observer (LESO) is used to estimate the system state variables and the total disturbances of the system. It is represented by the following model [13]:

$$\begin{cases} \dot{z} = Az + Bu + L(y - \hat{y}), \\ \hat{y} = Cz, \end{cases} \tag{25}$$

where z is the observed states vector, $z = \begin{bmatrix} z_1 & z_2 \end{bmatrix}^T$ (z_1 is the estimation of x_1 and z_2 is the estimation of x_2), $\hat{y}$ is the estimated output, and L is the observer gain vector defined as:

$$L = [2\omega_0 \quad {\omega_0}^2]^T, \tag{26}$$

ω_0 is determined by the placement of the poles in closed-loop to ensure both fast observer dynamics and minimal perturbations sensitivity.

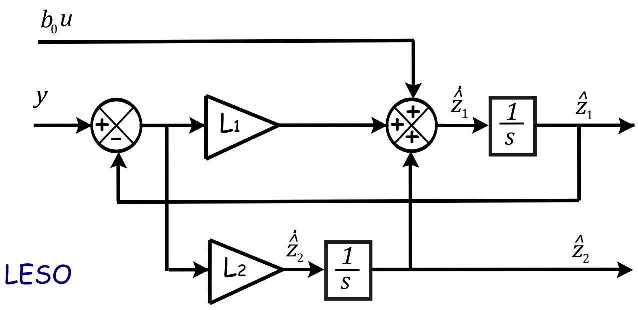

Fig. 5: Block diagram of a first order Linear Extended State Observer.

The control law of the system is:

$$u = \frac{u_0 - z_2}{b_0}, \tag{27}$$

where u_0 is a virtual controller. We suppose that z_2 is a correct estimation of $f (z_2 \approx f)$. By replacing Eq. (27) into Eq. (23) we obtain:

$$\begin{aligned} \dot{y} &= f + b_0 \frac{u_0 - z_2}{b_0}, \\ &= f - z_2 + u_0 \approx u_0. \end{aligned} \tag{28}$$

Therefore, the system Eq. (28) can be controlled by a proportional controller K_P.

$$u_0 = K_P(r - z_1) = K_P(r - \hat{y}), \tag{29}$$

r is the reference input signal to track.

The controller tuning is chosen as $K_P = \omega_c = 4/T_{settle}$, where T_{settle} is the closed loop desired settling time. ω_0 is taken as $\omega_0 = 3 \sim 7\omega_c$.

4. Control of the Machine Side Converter by LADRC

The MSC control is achieved by using the Linear Active Disturbance Rejection Controller that regulates the stator currents with its references, where Isd_{ref} is set to zero and Isq_{ref} is given by the Optimal Torque Control OTC-MPPT [19] block displayed in Fig. 6.

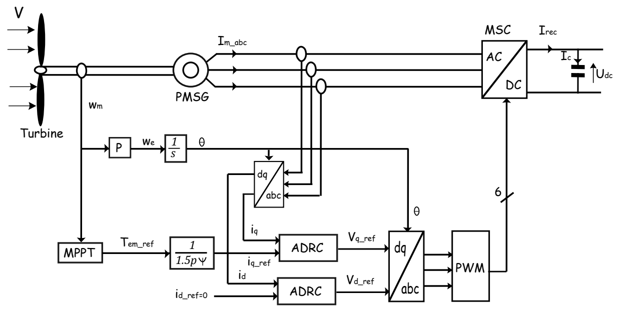

Fig. 6: Machine Side Converter Control by ADRC.

4.1. MPPT Analysis for Variable Wind Speed Turbine

To ensure maximum power extraction from the wind turbine, the rotational speed must be maintained at the optimum value of the tip speed ratio λ_{opt} which makes the turbine operating at $C_P = C_{P\max}$.

Considering the relationship between the wind speed V and the tip speed ratio λ in Eq. (4), the wind turbine power can be expressed as a function of the rotational speed Ω_m:

$$P_t = 0.5\rho\pi R^5 \frac{C_p(\lambda, \beta)}{\lambda^3} {\omega_m}^3. \tag{30}$$

Replacing λ by λ_{opt} and place in $C_p(\lambda, \beta) = C_{P\max}$, the wind turbine maximum power can be expressed as:

$$P_{t\max} = K_{opt} {\omega_m}^3, \tag{31}$$

where K_{opt} is a coefficient given by:

$$K_{opt} = 0.5\rho\pi R^5 \frac{C_{p\max}}{{\lambda_{opt}}^3}. \tag{32}$$

So the torque reference T_{em-ref} is expressed as follows:

$$T_{em-ref} = K_{opt} {\omega_m}^2. \tag{33}$$

4.2. LADRC Design for Machine Side Control

The Zero Direct axis Control (ZDC) is used to obtain the references of currents used in control [20]. The three phase stator currents is_{abc} are converted into d-q axis frame using Park's transformation technique, and then, the d-axis current i_d is to be set to zero and the q-axis current i_q is to be set equal to the stator current i_s.

$$i_s = \sqrt{{i_d}^2 + {i_q}^2} = i_q. \tag{34}$$

Consequently, for $i_d = 0$ the electromagnetic torque can be controlled by i_q:

$$T_{em} = \frac{3}{2} P \psi_f i_q. \tag{35}$$

Hence:

$$T_{em-ref} = \frac{3}{2} P \psi_f i_{qref}, \tag{36}$$

$$i_{qref} = \frac{2}{3P\psi_f} T_{em-ref}. \tag{37}$$

The stator currents regulations is achieved by two ADRC controllers, where the equations of i_d and i_q are adapted to the canonical from of ADRC.

$$\frac{\mathrm{d}y(t)}{\mathrm{d}t} = f(y, d, t) + b_0 u(t). \tag{38}$$

For the d-axis current we have:

$$\frac{\mathrm{d}i_d(t)}{\mathrm{d}t} = -\frac{R_s}{L_d} i_d + \omega_e i_q \frac{L_q}{L_d} + \frac{v_d}{L_d}, \tag{39}$$

where:

$$\begin{cases} f(y, d, t) = -\frac{R_s}{L_d} i_d + \omega_e i_q \frac{L_q}{L_d}, \\ b_0 = \frac{1}{L_d}, \\ u = v_d. \end{cases} \tag{40}$$

And for the q-axis we have:

$$\frac{\mathrm{d}i_q(t)}{\mathrm{d}t} = -\frac{R_s}{L_q} i_q - \omega_e i_d \frac{L_d}{L_q} - \frac{\psi_f}{L_q} + \frac{v_q}{L_q}, \tag{41}$$

and:

$$\begin{cases} f(y, d, t) = -\frac{R_s}{L_q} i_q - \omega_e i_d \frac{L_d}{L_q} - \frac{\psi_f}{L_q}, \\ b_0 = \frac{1}{L_q}, \\ u = v_q \end{cases} \tag{42}$$

5. Control of the Grid Side Converter by LADRC

The grid side converter is used to deliver the generated power into the electrical grid. The LADRC controller is used to stabilize the dc-link voltage and to adjust the active and reactive powers delivery into the grid during wind variations to achieve unity power factor. The GSC can be controlled either by Voltage Oriented Control (VOC) or Direct Power Control (DPC) technique. VOC is considered to be more efficient due to lower energy losses and to lower current distortion compared to DPC [21].

As illustrated in Fig. 7 , VOC is used to control the GSC and it involves a dual-loop control structure: an outer loop to control the DC link voltage and an inner loop to control the grid currents.

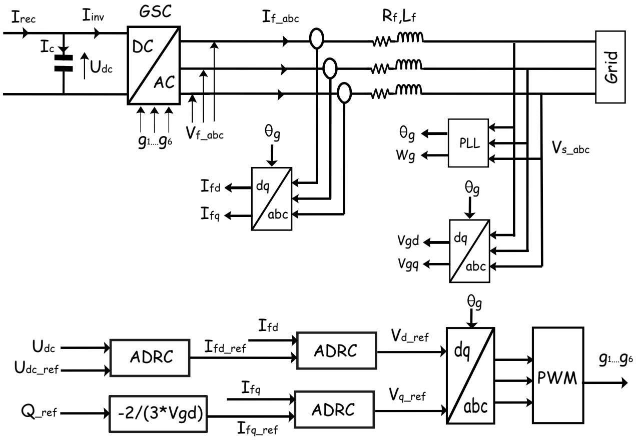

Fig. 7: Grid Side Converter Control BY ADRC.

The Phase Locked Loop device (PLL) is used to obtain the phase angle and frequency from the grid voltages [22]. The d-axis component of the synchronous reference frame is aligned with the grid voltage $v_{dg} = v_g$ and the q-axis component was set to zero $v_{qg} = 0$.
The active and reactive powers are then given by:

$$\begin{cases} P_g = \frac{3}{2} v_{gd} i_{fd}, \\ Q_g = -\frac{3}{2} v_{gd} i_{fq}. \end{cases} \tag{43}$$

5.1. DC Bus Voltage Control by LADRC

The power across the DC link Capacitor C, can be expressed by:

$$P_{dc} = U_{dc}(i_{rec} - i_{inv}). \tag{44}$$

By substituting Eq. (17) by Eq. (44), we get:

$$P_{dc} = C U_{dc} \frac{\mathrm{d}U_{dc}}{\mathrm{d}t}. \tag{45}$$

If all the losses in the filter,the power electronics converters, and in the capacitor are neglected, the exchanged powers on the DC bus are expressed by:

$$P_{dc} = P_m - P_g, \tag{46}$$

where P_m, P_g are the generator and grid powers respectively.

By taking into account Eq. (43), Eq. (44) and Eq. (45), the DC bus voltage can be expressed by:

$$CU_{dc}\frac{\mathrm{d}U_{dc}}{\mathrm{d}t} = U_{dc}i_{rec} - \frac{3}{2}v_{gd}i_{fd}. \tag{47}$$

Or:

$$\frac{\mathrm{d}{U_{dc}}^2}{\mathrm{d}t} = \frac{2U_{dc}}{C}i_{rec} - \frac{3v_{gd}}{C}i_{fd}. \tag{48}$$

We put $X = {U_{dc}}^2$:

$$\frac{\mathrm{d}X}{\mathrm{d}t} = \frac{2\sqrt{X}}{C}i_{rec} - \frac{3v_{gd}}{C}i_{fd}. \tag{49}$$

so we obtain:

$$\begin{cases} f(y,d,t) = \dfrac{2\sqrt{X}}{C}i_{rec}, \\ b_0 = -\dfrac{3v_{gd}}{C}, \\ u = i_{fd}. \end{cases} \tag{50}$$

5.2. Control of Filter Currents by LADRC

The external voltage regulation loop makes it possible to maintain the voltage across the capacitor U_{dc} and to generate the current reference i_{fd-ref} for the internal current loop.

For the current i_{fq-ref}, it is calculated by the desired delivery of reactive power.

$$i_{fq-ref} = -\frac{2}{3v_{gd}}Q_{f-ref}. \tag{51}$$

Then, similary to the machine side control, the filter currents are given in canonical form of ADRC.

For d-axis current:

$$\frac{\mathrm{d}i_{fd}}{\mathrm{d}t} = \frac{1}{L_f}(-R_f i_{fd} - v_{gd} + L_f\omega_g i_{fq}) + \frac{v_{fd}}{L_f}. \tag{52}$$

with:

$$\begin{cases} f(y,d,t) = \dfrac{1}{L_f}(-R_f i_{fd} - v_{gd} + L_f\omega_g i_{fq}), \\ b_0 = \dfrac{1}{L_f}, \\ u = v_{fd}. \end{cases} \tag{53}$$

For q-axis current:

$$\frac{\mathrm{d}i_{fq}}{\mathrm{d}t} = \frac{1}{L_f}(-R_f i_{fq} - L_f\omega_g i_{fd}) + \frac{v_{fq}}{L_f}. \tag{54}$$

with:

$$\begin{cases} f(y,d,t) = \dfrac{1}{L_f}(-R_f i_{fq} - L_f\omega_g i_{fd}), \\ b_0 = \dfrac{1}{L_f}, \\ u = v_{fq}. \end{cases} \tag{55}$$

6. Results and Discussion

To validate the theoretical study and the effectiveness of the presented control strategy, a complete structure of WECS composed of a variable speed wind turbine, a PMSG, and an electronic power converters connected to the grid are designed under MATLAB Simulink environment.

To examinate the tracking effectiveness of the proposed control, a variable wind speed profile is applied as shown in Fig. 8. The simulation parameters are given in App. A.

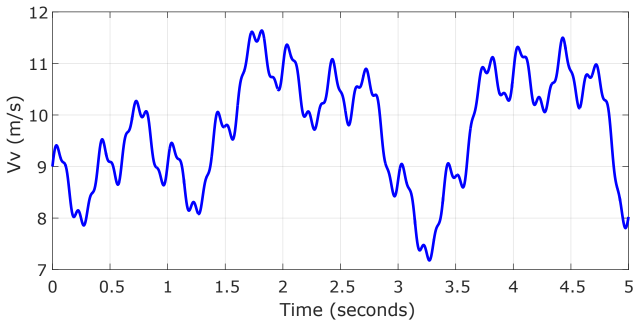

Fig. 8: Wind Speed Profile.

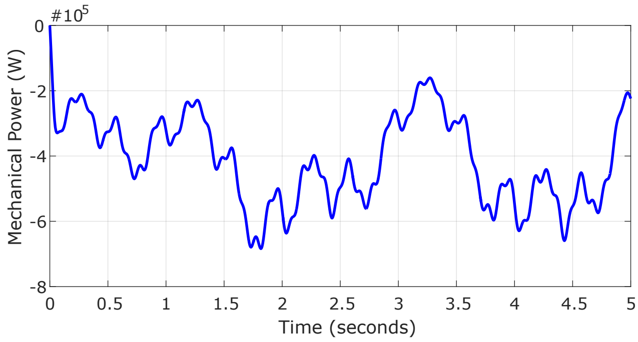

Fig. 9: Turbine Mechanical Power.

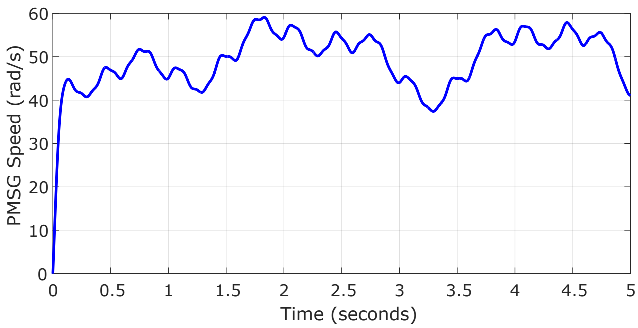

Fig. 10: PMSG Speed in rad·s^{-1}.

As can be noticed in Fig. 11, the power coefficient has been maintained at its optimal value ($C_{p\,\max} = 0.48$) which shows the effectiveness of the MPPT strategy in terms of maximum power extraction.

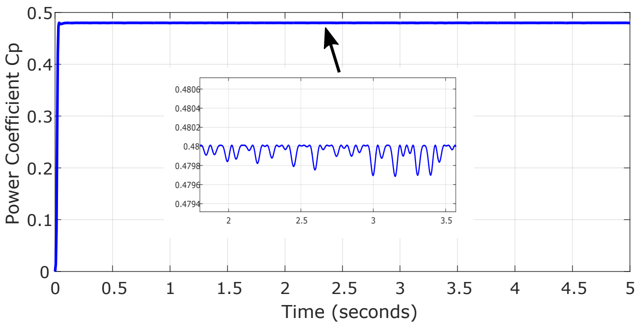

Fig. 11: Power Coefficient C_p.

The response of the linear ADRC shows a good tracking characteristics as highlighted in Fig. 12 and Fig. 13 where the direct axis current I_d was maintained to zero and the quadrature current I_q track its references. The generated currents are shown in Fig. 14.

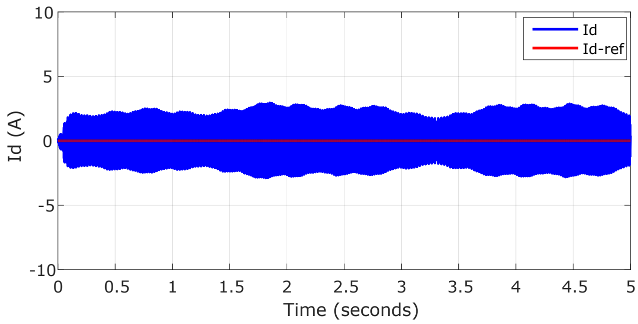

Fig. 12: Stator d-axis current I_d.

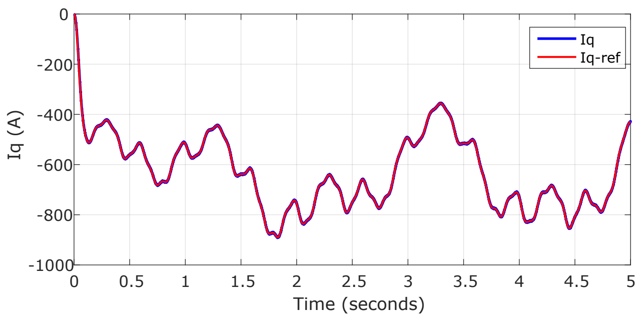

Fig. 13: Stator q-axis current I_q.

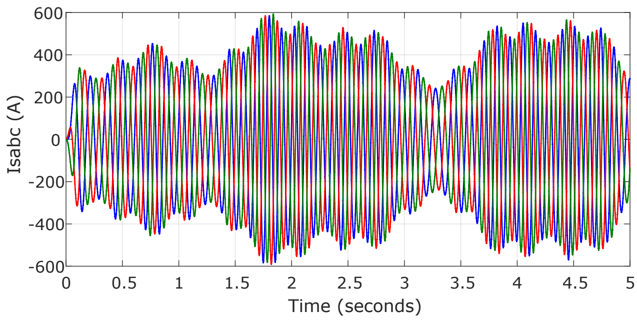

Fig. 14: PMSG Stator Currents Is_{abc}.

Figure 15 shows that the DC link voltage Vdc is maintained at its reference with some fluctuations which are due to the stochastic nature of wind speed. Also we notice in Fig. 16 and Fig. 17 that the linear ADRC regulates the grid currents to their references.

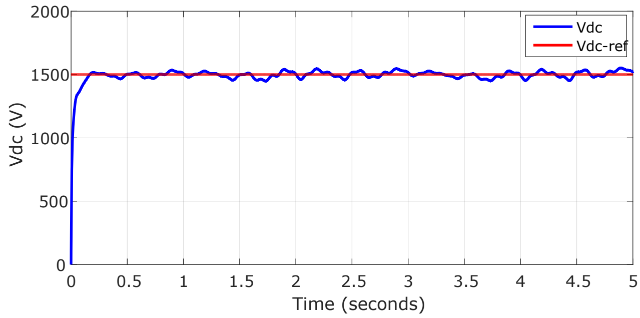

Fig. 15: DC Bus Voltage control by LADRC.

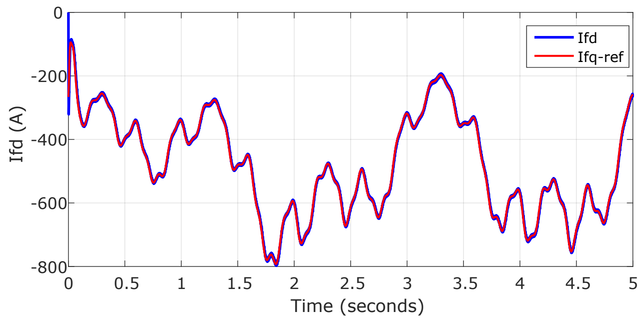

Fig. 16: Filter direct current I_{fd} control by LADRC.

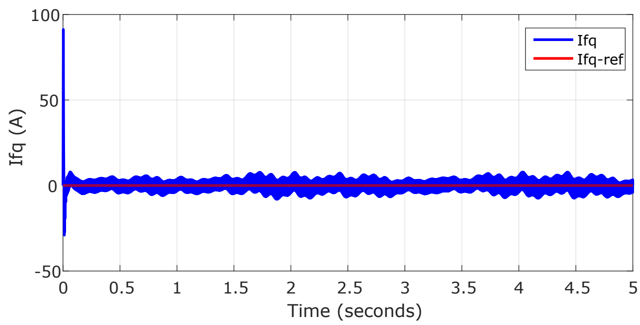

Fig. 17: Filter quadrature current I_{fq} control by LADRC.

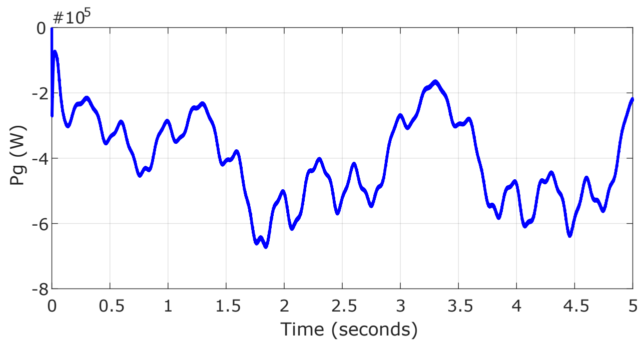

Fig. 18: Active power injected to the grid.

The control of the active and reactive powers is also achieved as shown in Fig. 18, Fig. 19, and Fig. 20 where the extracted power from the wind turbine was injected into the grid and the reactive power was set to zero to ensure a unit power factor.

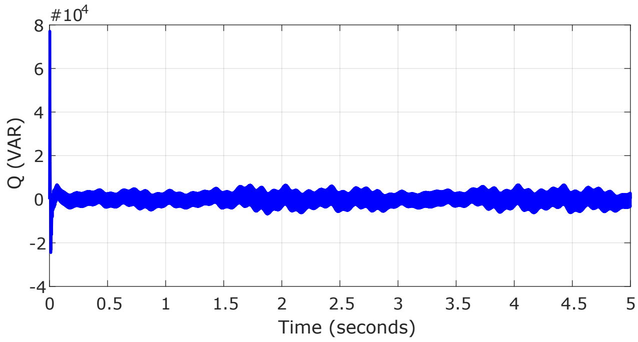

Fig. 19: Reactive power injected to the grid.

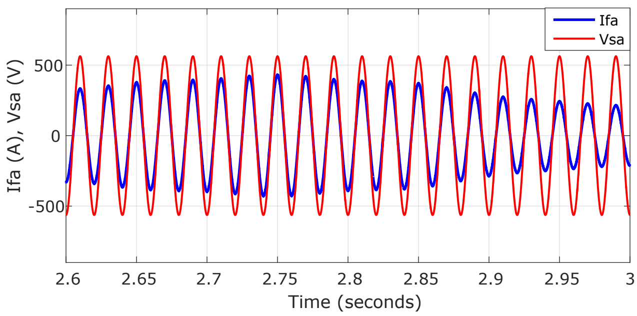

Fig. 20: Grid voltage Vs_a and Grid Current If_a.

In order to test the robustness of the proposed control strategy, another test was carried out in which we have changed the internal parameter of the PMSG, the stator indcutance L_s, by an increase of 50 % of the nominal value. The results obtained by LADRC are compared with the classical PI controller. The utilized wind speed profile is given in Fig. 21.

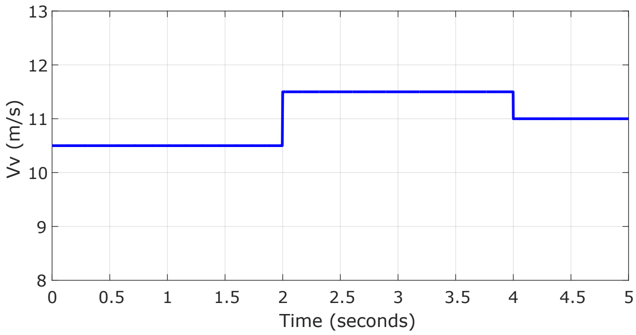

Fig. 21: Wind speed profile.

As shown in Fig. 22, both controllers regulate the current I_d to zero, but the LADRC controller has a faster response compared to the PI controller.

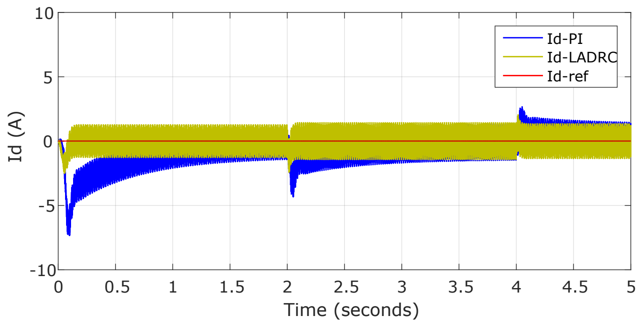

Fig. 22: Control of d-axis stator current I_d.

It can be noticed in Fig. 23 that the current I_q was regulated to its reference and that the response of LADRC is better than the PI one. Also, it can be observed in Fig. 24 that the DC bus voltage was regulated to its reference, where the LADRC does not show an overshoot as in the case of the PI control.

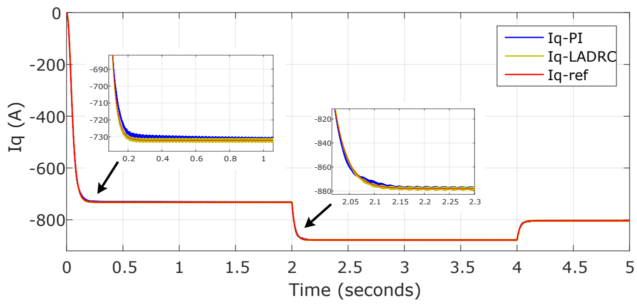

Fig. 23: Control of q-axis stator current I_q.

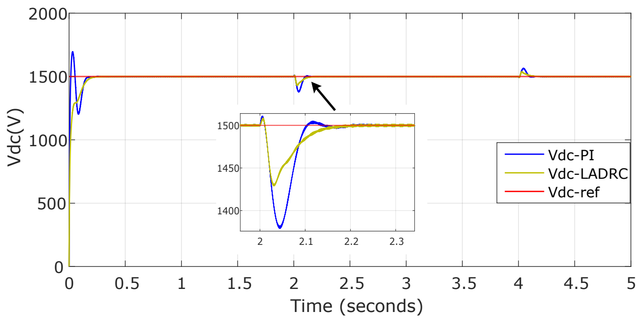

Fig. 24: Control of DC Bus Voltage V_{dc}.

So as a closing statement, the simulation results have demonstrated that the proposed strategy is efficient in terms of stability, rapidity, accuracy and for the robustness regarding the variation of the parameters of the machine.

7. Conclusion

This paper deals with the modelling and control of a wind energy conversion system based on a permanent magnet synchronous generator. A new control strategy has been proposed to operate the wind turbine with the aim to extract the maximum power from the wind energy and deliver it to the utility grid. This control strategy is known as the Active Disturbance Rejection Control. It has been presented and applied to the machine and the grid side converters. The objective consists in controlling the stator currents for adapting the PMSG rotational speed with the wind speed by acting on the electromagnetic torque of the generator (MPPT). The control of the active and the reactive powers was obtained by regulating the DC bus voltage and by controlling the grid currents according to their references.

The results have demonstrated that the suggested control strategy is efficient in terms of fast tracking and robustness for internal an external disturbances compared to the classical PI controller.

References

[1] PINTO, A. C., B. C. CARVALHO, J. C. OLIVEIRA, G. C. GUIMARAES, A. J. MORAES, C. H. SALERNO and Z. S. VITORIO. Analysis of a WECS Connected to Utility Grid with Synchronous Generator. In: *IEEE/PES Transmission Distribution Conference and Exposition*. Caracas: IEEE, 2006, pp. 1–6. ISBN 1-4244-0287-5. DOI: 10.1109/TDCLA.2006.311373.

[2] ZAHEDI, A. Current status and future prospects of the wind energy. In: *10th International Power Energy Conference (IPEC)*. Ho Chi Minh City: IEEE, 2012, pp. 54–58. ISBN 978-1-4673-4584-2. DOI: 10.1109/ASSCC.2012.6523238.

[3] ECHCHAACHOUAI, A., S. EL HANI, A. HAMMOUCH and I. ABOUDRAR. A Two-Level Sensorless MPPT Strategy Using SRF-PLL on a PMSG Wind Energy Conversion System. *Advances in Electrical and Electronic Engineering*. 2017, vol. 15, no. 3, pp. 383–390. ISSN 1804-3119. DOI: 10.15598/aeee.v15i3.2215.

[4] ERRAMI, Y., M. OUASSAID and M. MAAROUFI. Control of a PMSG based Wind Energy Generation System for Power Maximization and Grid Fault Conditions. *Energy Procedia*. 2013, vol. 42, iss. 1, pp. 220–229. ISSN 1876-6102. DOI: 10.1016/j.egypro.2013.11.022.

[5] DANG, C.-L., L. ZHANG and M.-X. ZHOU. Optimal Power Control Model of Direct Driven PMSG. *Energy Procedia*. 2011, vol. 12, iss. 1, pp. 844–848. ISSN 1876-6102. 10.1016/j.egypro.2011.10.111.

[6] MUDHOLKER, A., P. M. MENGHAL and A. J. LAXMI. SVPWM Based Converter for PMSG Based Wind Energy Conversion System. *Procedia Computer Science*. 2015, vol. 70, iss. 1, pp. 676–682. ISSN 1877-0509. DOI: 10.1016/j.procs.2015.10.104.

[7] HASSANZADEH, F., H. SANGRODY, A. HAJIZADEH and S. AKHLAGHI. Back-to-Back Converter Control of Grid-Connected Wind Turbine to Mitigate Voltage Drop Caused by Faults. In: *North American Power Symposium (NAPS)*. Morgantown: IEEE, 2017, pp. 1–6. ISBN 978-1-5386-2700-6. DOI: 10.1109/NAPS.2017.8107205.

[8] KASEM ALABOUDY, A. H., A. A. DAOUD, S. S. DESOUKY and A. A. SALEM. Converter Controls and Flicker Study of PMSG-Based Grid Connected Wind Turbines. *Ain Shams Engineering Journal*. 2013, vol. 4, no. 1, pp. 75–91. ISSN 2090-4479. DOI: 10.1016/j.asej.2012.06.002.

[9] BARROS, L. S. and C. M. V. BARROS. An Internal Model Control for Enhanced Grid-Connection of Direct-Driven PMSG-Based Wind Generators. *Electric Power Systems Research*. 2017, vol. 151, iss. 1, pp. 440–450. ISSN 0378-7796. DOI: 10.1016/j.epsr.2017.06.014.

[10] JING-QING, H. Auto Disturbance Rejection Controller and Its Applications. *Journal of Control and Decision*. 1998, vol. 13, no. 1, pp. 19–23. ISSN 2330-7706.

[11] JING-QING, H. Nonlinear Design Methods for Control Systems. *IFAC Proceedings Volumes*. 1999, vol. 32, iss. 2, pp. 1531–1536. ISSN 2405-8963. DOI: 10.1016/S1474-6670(17)56259-X.

[12] LI, S. and J. LI. Output Predictor-Based Active Disturbance Rejection Control for a Wind Energy Conversion System With PMSG. *IEEE Access*. 2017, vol. 5, iss. 1, pp. 5205–5214. ISSN 2169-3536. DOI: 10.1109/access.2017.2681697.

[13] SHI, Y.-T., K. QI, Q. SHU-JUAN, S. DE-HUI and L. ZHENG-XI. Optimal Control of PMSG Wind Energy Convert System Based on MPPT and ADRC Control Structure. In: *Proceedings of the 33rd Chinese Control Conference*. Nanjing: IEEE, 2014, pp. 6907–6912. ISBN 978-9-8815-6387-3. DOI: 10.1109/chicc.2014.6896138.

[14] LI, S., K. ZHANG, J. LI and C. LIU. On the Rejection of Internal and External Disturbances in a Wind Energy Conversion System with Direct-Driven PMSG. *ISA Transactions*. 2016, vol. 61, iss. 1, pp. 95–103. ISSN 0019-0578. DOI: 10.1016/j.isatra.2015.12.014.

[15] JAYALAKSHMI, N. S., D. N. GAONKAR and K. S. K. KUMAR. Dynamic modeling and

performance analysis of grid connected PMSG based variable speed wind turbines with simple power conditioning system. In: *IEEE International Conference on Power Electronics, Drives and Energy Systems (PEDES)*. Bengaluru: IEEE, 2012, pp. 1–5. ISBN 978-1-4673-4506-4. DOI: 10.1109/PEDES.2012.6484474.

[16] HAN, J. From PID to Active Disturbance Rejection Control. *IEEE Transactions on Industrial Electronics*. 2009, vol. 56, iss. 3, pp. 900–906. ISSN 0278-0046. DOI: 10.1109/TIE.2008.2011621.

[17] GUO, B., S. BACHA and M. ALAMIR. A Review on ADRC Based PMSM Control Designs. In: *IECON 2017 - 43rd Annual Conference of the IEEE Industrial Electronics Society*. Beijing: IEEE, 2017, pp. 1747–1753. ISBN 978-1-5386-1128-9. DOI: 10.1109/IECON.2017.8216296.

[18] HERBST, G. A Simulative Study on Active Disturbance Rejection Control (ADRC) as a Control Tool for Practitioners. *Electronics*. 2013, vol. 2, iss. 3, pp. 246–279. ISSN 2079-9292. DOI: 10.3390/electronics2030246.

[19] KUMAR, S. S., K. JAYANTHI and N. S. KUMAR. Maximum power point tracking for a PMSG based variable speed wind energy conversion system using optimal torque control. In: *International Conference on Advanced Communication Control and Computing Technologies (ICACCCT)*. Ramanathapuram: IEEE, 2016, pp. 347–352. ISBN 978-1-4673-9546-5. DOI: 10.1109/ICACCCT.2016.7831660.

[20] PORATE, D. K., S. P. GAWANDE, A. P. MUNSHI, K. B. PORATE, S. G. KADWANE and M. A. WAGHMARE. Zero Direct-Axis Current (ZDC) Control for Variable Speed Wind Energy Conversion System Using PMSG. *Energy Procedia*. 2017, vol. 117, iss. 1, pp. 943–950. ISSN 1876-6102. DOI: 10.1016/j.egypro.2017.05.214.

[21] MALINOWSKI, M., M. P. KAZMIERKOWSKI and A. TRZYNADLOWSKI. Review and comparative study of control techniques for three-phase PWM rectifiers. *Mathematics and Computers in Simulation, Modelling and Simulation of Electric Machines, Converters and Systems*. 2003, vol. 63, iss. 3–5, pp. 349–361. ISSN 0378-4754. DOI: 10.1016/S0378-4754(03)00081-8.

[22] DU, W., X. CHEN and H. WANG. PLL-Induced Modal Resonance of Grid-Connected PMSGs With the Power System Electromechanical Oscillation Modes. *IEEE Transactions on Sustainable Energy*. 2017, vol. 8, iss. 4, pp. 1581–1591. ISSN 1949-3029. DOI: 10.1109/TSTE.2017.2695563.

About Authors

Imad ABOUDRAR was born in Agadir, Morocco in 1993. He received the M.Sc. degree in electrical engineering in 2016 from the Mohammed V University, Rabat Morocco- where he is currently working towards the Ph.D. degree in the department of electrical engineering. Since 2016, his research interests are related to renewable energy, his current activities include the improvement of energy quality of an integrated PV and Wind Hybrid System connected to the grid.

Soumia EL HANI Professor of Electrical Machine and drives at the Ecole Normale Superieure de Enseignement Technique (ENSET), Mohammed V University Rabat, Morocco since 1992. She obtained her engineering degree From Higher school of Mines-Rabat, and her Ph.D. in Automatic from Mohammedia School of Engineering, Rabat Morocco in 2003. Her research interests are in the area of Robust Control, Monitoring and Diagnosis of Electromechanical Systems. She is in charge of the research team Energy Optimisation, Diagnosis and Control' EODIC, research Laboratory in Energy, Electrotechnic, Robotic and Automatic. She is Author of several publications in the field of electrical engineering, including robust control systems, diagnosis and control systems of wind electric conversion. She has supervised Ph.D. and Masters Theses dealing with different research topics concerned with her research interests. Soumia El Hani is Prof. Dr. IEEE senior member, she was a member of the Organizing and the Scientific Committees of several international conferences dealing with topics related to Renewable Energy, Electrical Machines and Drives. Since the year 2015, Soumia El Hani is the co-founder and general co- chair of The International Conference on Electrical and Information Technologies. Also, she is the co-editor of ICEIT 2015, ICEIT 2016, and ICEIT 2017 Proceedings.

Hamza MEDIOUNI was born in Khourigba, Morocco, in 1993. He received the M.S. degree in electrical engineering in 2016 from the Mohammed V University in Rabat- Morocco. Where he is currently working towards the Ph.D. degree in the department of electrical engineering. Since 2017, His research interests are related to electrical machines and drives control.

Ahmed AGHMADI was born in Jeddah, Saudi Arabia. He received his B.Sc. degree from the Superior School of Technology, Hassan 1st University, Settat, Morocco in 2015 and M.Sc. degree in Electrical Engineering from Mohamed 5th University, Morocco in 2017. He is currently a Ph.D. candidate at The Energy Optimization, Diagnosis and Control Research

Laboratory at Electrical Engineering Department, Ecole Normale Suprieure de l'Enseignement Technique, Mohamed 5th University, Rabat, Morocco. His current research interests are Smart grids, Renewable Energy Systems, Optimization and Mangament of hybrid energy systems and Hybrid AC/DC Power Systems.

Appendix A PMSG Wind Turbine Parameters

- Radius: $R = 24$ m,
- Nominal wind speed: $V_v = 12$ m·s^{-1},
- Total inertia of the mechanical transmission: $J_T = 10^5$ kg·m^2,
- $C_{Pmax} = 0.48$,
- $\lambda_{optimal} = 8.1$,
- Nominal power: $P_n = 750$ kW,
- Stator resistance: $R_s = 6.52 \cdot 10^{-3}$ Ω,
- Stator inductance: $L_s = L_d = L_q = 3.85 \cdot 10^{-3}$ H,
- Flux: $\Psi = 8.53$,
- Pair poles: $P = 26$,
- DC bus voltage: $V_{dc} = 1500$ V,
- DC bus Cpacitor: $C = 5000 \cdot 10^{-6}$ F,
- Filter Resistance: $R_f = 0.1$ Ω,
- Filter Inductance: $L_f = 2 \cdot 10^{-3}$ H.